

## BEARING CAPACITY OF SPREAD FOUNDATIONS ON SAND OVERLYING CLAY

K. Yamamoto<sup>1</sup> and D. Kim<sup>2</sup>

**ABSTRACT:** The ultimate bearing capacity of spread foundations on a sand layer overlying clay has been extensively investigated for practical use. First, a review of previous studies on bearing capacity problems for this type of foundation has been performed and a discussion is presented concerning the application to practice. Second, the kinematic approach of limit analysis has been used to calculate the upper bound of the true ultimate bearing capacity. The kinematic solutions are upper bounds and their accuracy depends primarily on the nature of the assumed failure mechanism. This approach makes it convenient to create design charts, and it is possible to trace the influence of parameters. Third, the commercial finite element program ABAQUS was applied to obtain the ultimate bearing capacity based on the elasto-plastic theory. Although FE analysis has still not gained wide acceptance in foundation practice, FE analysis has the great advantage in which the equations of equilibrium and compatibility are solved together, compared with limit analysis. Finally, results obtained from the kinematic approach and the program ABAQUS were compared with those from the existing limit equilibrium equations proposed by Yamaguchi, Meyerhof and Okamura et al. for confirming the validity of their application to practice.

**Key Words:** Foundations, bearing capacity, limit analysis, finite element method, limit equilibrium method

### INTRODUCTION

Ultimate bearing capacity and the failure mechanism of shallow foundations on a homogeneous soil layer have been largely investigated to date since the conventional bearing capacity theory proposed by Terzaghi (1943). Shallow foundations are sometimes located in a sand layer with limited thickness on a deep clay bed. In practice, the bearing capacity of foundations on soft clay is often improved artificially by placing a sand layer on the clay. Even in natural soils, there are many cases where the soil properties vary with the depth. The bearing capacity and failure mechanism of such nonhomogeneous soil profiles still remain unclear due to the relative difficulty of obtaining exact solutions, compared with a homogeneous soil. Therefore, the purpose of this paper is to investigate the specific case of a rigid foundation on the surface of a uniform sand layer overlying a homogeneous bed of clay and to solve these bearing capacity problems using several approaches for the application to

practice. Although the strength properties of the upper sand layer and the lower clay are quite different, each layer is often assumed to be homogeneous. Recently, the finite element method (FEM) has been recognized as a very effective tool to study inhomogeneous soils like two-layer foundation soils, because it can account for complex boundary conditions and soil inhomogeneity. In performing FE analysis, however, rich experience and some trial-and-error is required for discretization as well as selection of an analytical method, model and soil parameters. For this reason, FEM has still not gained wide acceptance in foundation design practice. In addition, for problems like two-layer foundation soils, convergence may be difficult to achieve.

The ultimate bearing capacity of foundations on a sand layer overlying clay has been mainly estimated by small-scale model tests and limit equilibrium methods. Yamaguchi (1963) first proposed the load spread mechanism, in which the load below the foundation is assumed to be spread uniformly over the top of the clay layer and that the foundation fails

---

<sup>1</sup> Research Associate, Department of Ocean Civil Engineering, Kagoshima University, Kagoshima 890-0065, JAPAN

<sup>2</sup> Research Engineer, Indiana Department of Transportation (INDOT), West Lafayette, IN, 47906-279, USA

Note: Discussion on this paper is open until June 1, 2005

due to a bearing capacity failure within the clay, as shown in Fig. 1. This approach is widely known as a simplified calculation of the bearing capacity. The load spreading angle  $\alpha$  to the vertical plane in Fig. 1 is always constant ( $\alpha = 30^\circ$ ), regardless of the strength parameters ( $\phi$  and  $c_u$ ) of two-layer foundation soils and  $H/B$ . Although the value of  $\alpha$  is an important factor for the calculated bearing capacity, it still remains unclear which value of  $\alpha$  is suitable. As a characteristic of this approach, it is useful for understanding the mechanics of the problem intuitively. Meyerhof (1974), Hanna and Meyerhof (1980), and Hanna (1981) proposed the punching shear mechanism as shown in Fig. 2, in which a sand block having vertical sides is assumed to be pushed into the clay together with the foundation. The sand is also assumed to be in a passive condition and the bearing capacity is obtained from the equilibrium condition of the sand block. In this approach, a punching shear coefficient  $K_s$  is introduced to consider conveniently the passive force on a vertical plane below each edge of the foundation. Typical punching shear coefficients for the punching shear mechanism can be found in their papers. Hanna and Meyerhof (1980) presented the values of  $K_s$  corresponding to each friction angle  $\phi$  as a function of the undrained shear strength of clay and the punching shear parameter  $\delta/\phi$ . They presented the cases only for high friction angle  $\phi = 40, 45, \text{ and } 50^\circ$  and these charts are not shown in nondimensional form. In the series of research by Meyerhof and Hanna, since the design charts for  $K_s$  are not shown in nondimensional form, the application to practice is quite restricted.

Kraft and Helfrich (1983) reported that the method developed by Hanna and Meyerhof (1980) provides good estimates of the bearing capacity of shallow foundations, and the projected area method using a load distributed with 2V:1H should not be used in comparison with measured results of full-scale and model bearing capacity tests. Kenny and Andrawes (1997) discussed load spreading analysis for a sand layer overlying clay based on data from a model loading test. They proposed a load spreading angle depending only on the bearing capacity ratio ( $q_c/q_u$ ) and a polynomial function of the ratio of applied footing stress and ultimate bearing capacity ( $q/q_u$ ) and the normalized settlement ( $S/B$ ). However, it is difficult to apply their results to practice since there is a deficiency in the general approach proposed (Burd

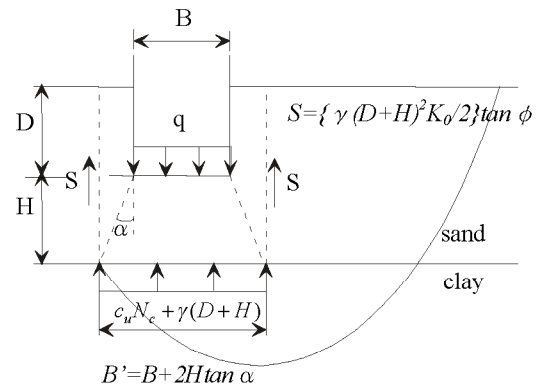


Fig. 1 Load spread mechanism proposed by Yamaguchi (1963)

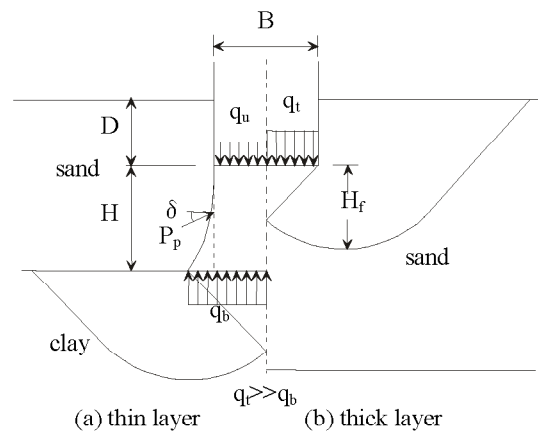


Fig. 2 Punching shear mechanism proposed by Meyerhof (1974)

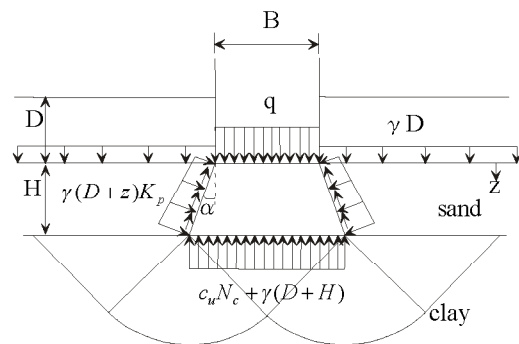


Fig. 3 Failure mechanism assumed by Okamura et al. (1998)

and Frydman 1999). Also, it would be difficult to propose accurately the load spreading angle for any particular case. Additionally, because of the scale effect of bearing capacity, a series of centrifuge model loading tests on dense sand overlying soft clay were carried out to investigate ultimate bearing capacity and associated deformations including the failure mechanism (Okamura et al. 1997). Okamura et al. (1998) proposed a failure mechanism shown in Fig. 3, based on the results of the centrifuge tests and derived newly the bearing capacity equation using the limit equilibrium method. In this mechanism, the vertical stress on the base of the sand block was assumed to be the ultimate bearing stress of a rigid foundation with rough base on the clay subjected to a surcharge pressure. It was also assumed that the load spreading angle within the upper sand layer changes with both varying strength parameters in the two soil layers and the ratio of the depth of sand below the foundation to the width of the foundation,  $H/B$ . The main difference of the bearing capacity equations proposed by Yamaguchi and Okamura et al. using load spread mechanism is the assumptions of  $\alpha$  and the shearing resistance acting on the sides of the sand block in the sand layer. Since the centrifuge tests provide nearly the same stress level as that in the prototype, the results obtained from the centrifuge tests would be more realistic than those from small gravitational tests. Moreover, they have obtained relatively good agreement between measured bearing capacity and calculated one. It is therefore considered that the ultimate bearing capacity calculated by Okamura et al. can be regarded to be most accurate among above limit equilibrium methods. Notice that all limit equilibrium methods proposed by Yamaguchi (1963), Meyerhof (1974), Hanna and Meyerhof (1980), Hanna (1981) and Okamura et al. (1998) lack rigor, neither the equilibrium condition nor the compatibility condition are guaranteed there.

Burd and Frydman (1997) investigated the bearing capacity of sand layers overlying clay using both finite element and finite difference methods to make the consistency and reliability of their results. They illustrated the mechanics of the system, the effectiveness of the sand layer for spreading the footing load. Also, they showed that a load spreading angle increases with increasing sand friction angle, and tends to reduce significantly when the shear strength of the clay increases. Referring to the bearing capacity equation proposed by Okamura et al. (1998),

Mizuno and Tsuchida (2002) calculated the ultimate bearing capacity on a sand layer overlying clay using elasto-plastic FEM. They reported that FEM solutions and the ultimate bearing capacities calculated by Okamura et al. agreed well, regardless of the variation of  $H/B$ . In their analytical conditions, they considered an undrained shear strength of  $100 \text{ kN/m}^2$  for the clay layer, which is quite large compared with the typical clay foundation. Moreover, neither the outline of the analytical method nor the bearing capacity vs. settlement curves from their FEM analysis was given. Therefore, it remains unclear how they obtained the ultimate bearing capacity from their analysis. Michalowski and Shi (1995) applied the upper bound analysis to several combinations of two-layer foundations soil where the foundation rests on a sand layer overlying clay. They showed that the depth of the failure mechanism is very dependent on the strength of the clay. The results were presented in the form of useful design charts that cover a broad range of parameters. They also considered a relatively hard clay rather than a weak one. They neither presented the bearing capacity equation for two-layer foundation soils derived from the upper bound theory and another failure mechanism where the failure is entirely contained within the upper sand layer, nor compared adequately the upper bound solutions with other solutions derived from other methods for the validity of practice use. They compared some solutions with those derived from other methods only for the case of high internal friction angle,  $\phi \geq 40^\circ$ .

The objective of this paper is to investigate the ultimate bearing capacity of spread foundations on a sand layer overlying clay using several approaches for the application to practice. First, upper bound analysis was applied to calculate the upper bound of the true ultimate bearing capacity for this type of problem, similar to the approach proposed by Michalowski and Shi (1995). Next, the commercial finite element program ABAQUS (HKS 2001) was also used to obtain the ultimate bearing capacity based on elasto-plastic theory. Finally, results obtained from the upper bound analysis and the program ABAQUS were compared with those from the limit equilibrium equations proposed by Yamaguchi (1963), Meyerhof (1974) and Okamura et al. (1998) for confirming the validity of their application to practice.

PROBLEM TO BE ANALYZED

This paper is concerned with the specific problem of the bearing capacity of spread foundations on a sand layer overlying clay. The analytical conditions adopted in this paper are shown in Fig. 4, in which B is the width of foundation and H is the depth of a sand layer below the foundation. In the calculation of bearing capacities, B=1.0 m and a unit weight of  $\gamma = 20 \text{ kN/m}^3$  for the sand were used. The values of the internal friction angle  $\phi$  for the sand were  $30^\circ$ ,  $35^\circ$  and  $40^\circ$ , and the values of cohesion  $c_u$  for the clay were 10, 30, and 50  $\text{kN/m}^2$ . Each layer was assumed to be homogeneous. Values of ratio H/B included H/B=0, 1, 2, 3, and 4. It is noted that H/B=0 and H/B=5 indicate uniform clay and sand soils, respectively. The case of a rigid foundation with rough base was considered. In this paper, the conditions shown in Fig. 4 are analyzed using the existing limit equilibrium method, upper bound analysis and finite element analysis.

UPPER BOUND ANALYSIS

Limit analysis is a convenient mathematical tool for estimating the bearing capacity of foundations. The upper bound theorem states that if the velocity (or strain rate) field is unstable (i.e., the rate of external work calculated from the velocity (or strain rate) field exceeds or equals the internal power dissipation) and kinematically admissible (i.e., the strain rate field is compatible with the velocities at the boundary of the soil mass), then collapse is either imminent or underway; that is, the true collapse load is definitely less than or at most equal to the load calculated from such a condition (e.g. Chen 1975;

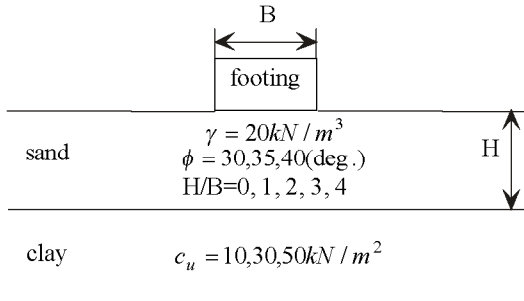


Fig. 4 Analytical conditions adopted in this paper

Chen and Liu 1990). The upper bound theorem satisfies the flow rule (the constitutive relation of the material), the compatibility condition and the velocity boundary conditions, but not the equilibrium condition. Based on the failure mechanism proposed by Michalowski and Shi (1995), the failure mechanism as shown in Fig. 5(a) was set up. In the case of the general shear failure, it is considered that this mechanism would be a suitable representation of the real failure mechanism. In Fig. 5(a),  $\alpha$  is the angle of the side to the vertical in the sand block,  $l$  is the depth of the failure mechanism,  $V_i$  is the kinematically admissible velocity vector and  $[V]_i$  is the velocity-jump vector along discontinuities. The mechanism is symmetrical and the region oeba moves downward as a rigid body at the same velocity  $V_0$  as the foundation. The downward movement is transmitted as the transversal movement of the fan region bcd. Consequently, the movement of the region bcd is transmitted as the upward movements of both the region abdc and triangular region acf. Upward is the negative direction. The upper bound of the true ultimate bearing capacity can be calculated by the following energy balance equation:

$$2E_{bc} + 2E_{bcd} + 2E_{cd} + 2E_{de} = 2W_{opba} + 2W_{pcb} + 2W_{bcd} + 2W_{bde} + 2W_{abe} + 2W_{aef} + W_{foot} \quad (1)$$

where  $E_{bc}$  and  $E_{bcd}$  are the internal power dissipations in a velocity discontinuity bc and within the continually deforming region bcd,  $W_{opba}$  and  $W_{foot}$  are the rate of external work due to region opba and the load from the foundation, respectively. In Eq. (1), the total internal power dissipation  $E_{total}$  along all velocity discontinuities is equal to the total rate of external work  $W_{total}$  in the mechanism. Since the associated flow rule is used, the internal power dissipation along the velocity discontinuities in the upper sand layer is zero. In the clay, the internal power dissipation is calculated as the product of the value of the cohesion and the magnitude of the velocity-jump vector. By solving Eq. (1), the specific expression for the upper bound  $q_0$  of the true ultimate bearing capacity can be written as

$$\frac{q_0(\xi, \eta, \alpha)}{c_u} = N_c(\xi, \eta, \alpha) + GN_\gamma(\xi, \eta, \alpha), \quad G = \frac{\gamma B}{2c_u} \quad (2)$$

$$N_c(\xi, \eta, \alpha) = \frac{\cos(\alpha + \beta) \cos \xi \cos \eta}{\cos(\alpha + \beta) \cos \xi \cos \eta - \sin \alpha \sin \beta} \{ \tan \xi + 2(\pi - \xi - \eta) + \tan \eta \} \quad (3)$$

$$N_\gamma(\xi, \eta, \alpha) = \frac{\cos \alpha \sin \beta}{2 \{ \cos(\alpha + \beta) \cos \xi \cos \eta - \sin \alpha \sin \beta \}^2} \times \{ \sin \alpha \sin \beta - \cos \xi \cos \eta \cos(\alpha + \beta) \} + \frac{\sin \beta \cos \beta \cos \xi \cos \eta \cos(\beta - \eta) \cos^2 \alpha}{2 \cos(\beta + \alpha) \{ \cos(\alpha + \beta) \cos \xi \cos \eta - \sin \alpha \sin \beta \}^2} \quad (4)$$

The upper bound  $q_0$  is independent of the specific weight of the clay. In the case of obtaining the upper bound value using Eqs. (2)-(4), the values of three parameters  $\xi$ ,  $\eta$  and  $\alpha$  have to be determined to take the minimum value of  $q_0$  in Eq. (2). Therefore, when the following conditions are satisfied,  $q_0(\xi, \eta, \alpha)$  takes the minimum value.

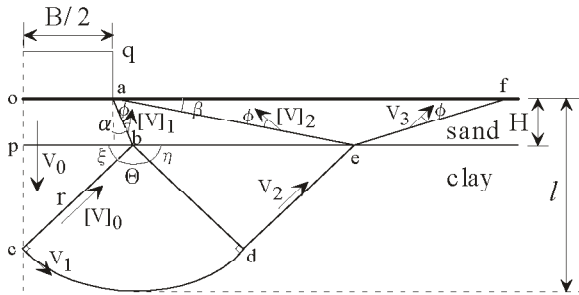
$$\frac{\partial q_0}{\partial \xi} = 0, \frac{\partial q_0}{\partial \eta} = 0, \frac{\partial q_0}{\partial \alpha} = 0 \quad (5)$$

Accordingly, the upper bound value  $q$  can be expressed as

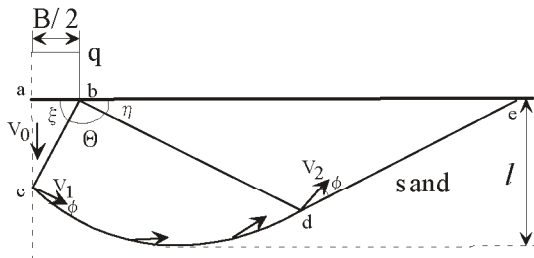
$$q = \min q_0(\xi, \eta, \alpha) \quad (6)$$

Since it is very difficult to obtain analytical solutions using Eq. (5), all possible combinations of  $\xi$ ,  $\eta$  and  $\alpha$  satisfying a kinematically admissible velocity field are considered in order to take the minimum value of the upper bound. Parameters  $\Theta$  and  $\beta$  in Fig. 5(a) can be found based on the geometric conditions, after values of  $\xi$ ,  $\eta$  and  $\alpha$  are set.

The bearing capacity generally increases with the depth of upper sand layer. As the upper sand layer becomes relatively thick, the failure will be fully contained within the upper sand layer. Thus, it is needed to obtain the upper bound solutions calculated by the failure mechanism within the uniform sand layer. The failure mechanism within the uniform sand layer used in this paper is assumed as shown in Fig. 5(b). The mechanism is symmetrical and the logarithmic spiral is used for the region bed. Like the above procedure, the upper bound  $q_0$  for the uniform sand layer is as follows:



(a) Two-layer foundation soil



(b) Uniform sand layer

$$q_0(\xi, \eta) = \frac{\gamma B}{2} N_\gamma(\xi, \eta) \quad (7)$$

$$N_\gamma(\xi, \eta) = \frac{-\tan \xi}{2} + \frac{\cos(\xi - \phi)}{2 \cos^2 \xi \cos \phi (1 + 9 \tan^2 \phi)} \times \{ 3 \tan \phi \cos \eta - \sin \eta \} \exp[3(\pi - \eta - \xi) \tan \phi] + 3 \tan \phi \cos \xi + \sin \xi \} + \frac{\cos(\xi - \phi) \sin \eta \cos \eta \exp[3(\pi - \eta - \xi) \tan \phi]}{2 \cos^2 \xi \cos(\eta + \phi)} \quad (8)$$

Therefore, the upper bound value  $q$  can be expressed as

$$q = \min q_0(\xi, \eta) \quad (9)$$

All possible combinations of  $\xi$  and  $\eta$  satisfying a kinematically admissible velocity field are considered in order to take the minimum value of the upper bound.

Fig. 5 Failure mechanism assumed in upper bound analysis

FINITE ELEMENT ANALYSIS

The finite element method can be employed to analyze the ultimate bearing capacity of two-layer foundation soils and obtain an accurate approximation of the true ultimate bearing capacity. Although there are many sources of errors such as the discretization of the continuum by finite elements, the solution scheme and its incrementation, it is considered that careful handling of the sources of error makes the results of finite element analysis closer to the exact solution. The commercial finite element program ABAQUS (HKS 2001) was used to analyze the ultimate bearing capacity. ABAQUS solves problems with material non-linearity effectively by employing a Newton-Raphson iterative scheme with automatic incrementation.

Method of Analysis

In the analysis, both clays and sands are modeled using the Drucker-Prager model. Unlike the Mohr-Coulomb criterion, the Drucker-Prager model considers the influence of the intermediate principal stress (Chen and Saleeb 1994). In addition, the Drucker-Prager model is mathematically convenient to use in three-dimensional applications, as it generates a smooth failure surface in stress space (Desai and Siriwardane 1984). In terms of the stress invariants  $I_1$  and  $J_2$ , the Drucker-Prager model without cap can be written as:

$$f(I_1, J_2) = \sqrt{J_2} - \alpha I_1 - k = 0 \tag{10}$$

where  $I_1$  and  $J_2$  are the first invariant of the stress tensor and the second invariant of the deviator stress tensor, respectively, and  $\alpha$  and  $k$  are model parameters that can be related to the Mohr-Coulomb strength parameters  $c$  and  $\phi$  for plain strain conditions. In finite element analysis, the selection of boundary conditions, mesh size and fineness are important factors for obtaining reasonable results. In the analyses, the effects of these factors were thoroughly investigated in the plane-stain (2D) analyses to determine a reasonable depth and width. Figure 6 shows a typical finite element mesh. The mesh was composed of four-node, second-order, plane-strain quadrilateral elements. The FE model was set in symmetry. In this figure, the analytical condition is

$H/B=1$  and the number of elements is 3600. The bottom boundary of the mesh was fixed and the lateral boundaries were modeled with rollers. The bottom and lateral boundaries were placed far enough not to influence the bearing capacity and failure mechanism. Every mesh used in the analysis was made fine near the edge of the foundation. In every case, we tried to use a finer mesh composed of eight-node quadrilateral elements, but, following convergence problems, we adopted four-node quadrilateral elements. The foundation was modeled as a rigid foundation with rough base, in which all of the nodes under the footing have the same displacement. The soil was modeled with an associated flow rule (the yield function is equal to the plastic potential function) to facilitate the numerical solution. In order to obtain ultimate bearing capacity values, a vertical displacement was applied to the nodes below the footing while its horizontal displacement was constrained to zero. The total load was obtained as the vertical reaction force below the footing. The average footing pressure was then obtained by dividing the vertical load by the width of the footing. In general, the load-settlement curves obtained from FE analysis do not always show a distinct point for determining of ultimate bearing capacity. The characteristics of curves depend on the failure mode such as general, local or punching shear failure. Initially, the bearing capacity of the footing was defined as the load at  $S/B=0.10$ , where  $S$  and  $B$  are the settlement and the width of the foundation. In some of the cases, however, a continuous increase in bearing capacity was observed even at  $S/B=0.10$ .

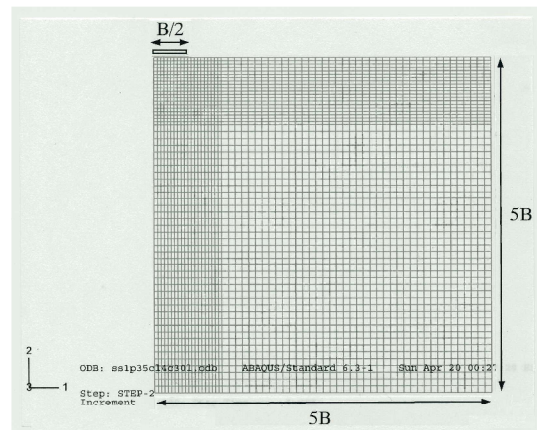


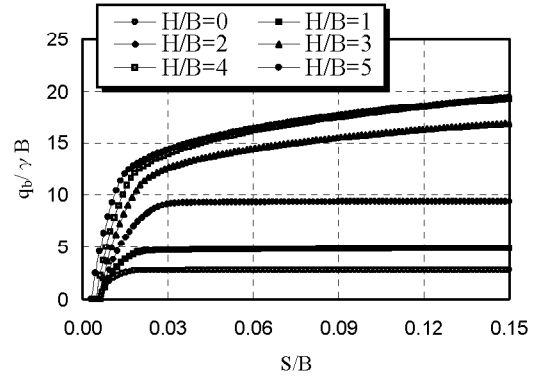
Fig. 6 Finite element mesh

Therefore, the vertical displacements were applied up to  $S/B=0.15$ . Although it requires some degree of judgment and experience for determining ultimate bearing capacity from load-settlement curve, the ultimate bearing capacity is defined using the load at  $S/B=0.15$  as one of the criteria in the analysis. In order to consider more realistic stress conditions in the soils, the FE analysis consists of two steps: geostatic stress analysis and main analysis. The geostatic analysis is performed to account for the initial stress condition of the soils. After the geostatic step is completed, the vertical displacement of the foundation is generated in the main analysis. The gravity loading of the soils induces small deformations in the geostatic stress analysis. Thus, small settlements exist prior to the main analysis. The total settlement in the analysis is defined as the settlement occurring in both the geostatic stage and the loading stage. According to several preliminary analyses using varying elastic moduli ( $E$ ) and Poisson's ratios ( $\nu$ ), it was noted that as the elastic modulus increases, the slope of the load-settlement increases but it does not affect the ultimate bearing capacity, provided  $E$  and  $\nu$  are in a reasonable range.

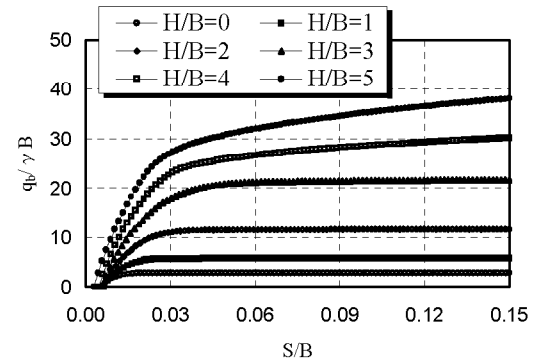
Results of Analysis

Figure 7 shows the relationship between the normalized footing pressure  $q_b/\gamma B$  and the normalized settlement  $S/B$  for two-layer foundation soils. It is noted that  $q_b$  is the footing pressure at the base of foundation. The internal friction angles of the sand layer were  $30^\circ$ ,  $35^\circ$  and  $40^\circ$ , and the normalized cohesion  $c_u/\gamma B$  was 0.5 for the three cases. From Figs. 7(a)-(c), as the normalized depth of a sand layer  $H/B$  increases,  $q_b/\gamma B$  also increases. It is seen that  $q_b/\gamma B$  tends to converge to a constant value, as  $S/B$  increases for  $H/B=0, 1$  and  $2$  in Fig. 7(a), for  $H/B=0, 1, 2$  and  $3$  in Fig. 7(b) and for  $H/B=0, 1, 2, 3$  and  $4$  in Fig. 7(c). Except for the above cases,  $q_b/\gamma B$  increases gradually even at  $S/B=0.15$ . The condition  $H/B=5$  indicates the case of only a sand soil. As  $\phi$  increases, the difference of bearing capacity between  $H/B=4$  and  $5$  becomes larger. It is found from Figs. 7(a)-(c) that for high values of internal friction angle  $\phi$  in the sand layer,  $\phi$  has more influence on the increase of bearing capacity in two-layer foundation soils.

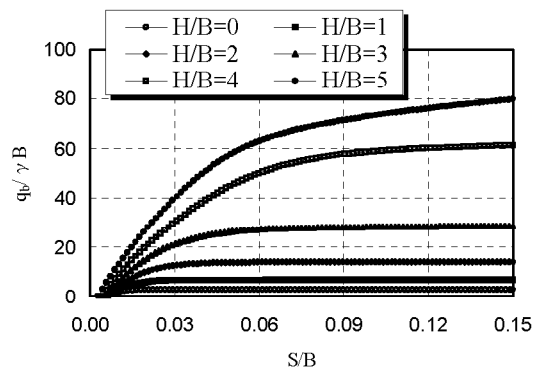
Figure 8 shows the same relationship as Fig. 7, in which the internal friction angle of the sand was fixed



(a)  $\phi = 30^\circ$ ,  $c_u/\gamma B = 0.5$

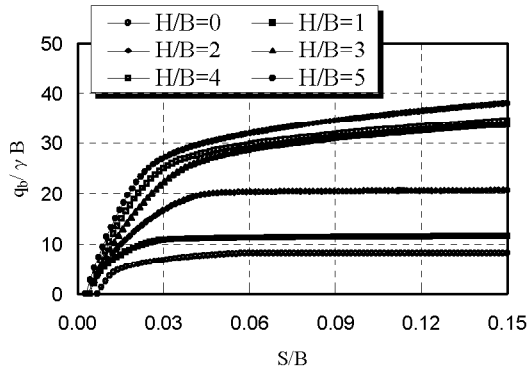


(b)  $\phi = 35^\circ$ ,  $c_u/\gamma B = 0.5$

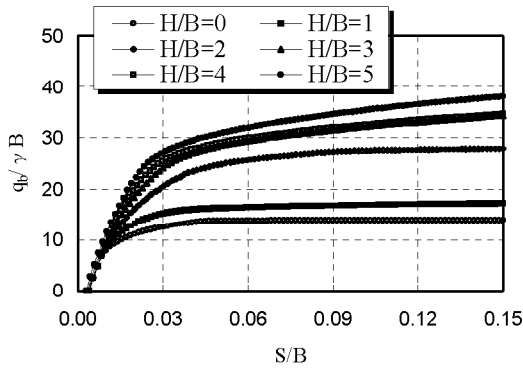


(c)  $\phi = 40^\circ$ ,  $c_u/\gamma B = 0.5$

Fig. 7 Relationship between  $q_b/\gamma B$  and  $S/B$  from finite element analysis



(a)  $\phi = 35^\circ$ ,  $c_u / \gamma B = 1.5$



(b)  $\phi = 35^\circ$ ,  $c_u / \gamma B = 2.5$

Fig. 8 Relationship between  $q_b / \gamma B$  and  $S/B$  from finite element analysis

( $\phi = 35^\circ$ ), and  $c_u / \gamma B$  was 1.5 and 2.5 for the two cases. From Fig. 7(b) and Figs. 8(a) and (b), when the normalized cohesion  $c_u / \gamma B$  is larger, the starting points between  $q_b / \gamma B$  and  $S/B$  become almost the same. In Fig. 8, as  $S/B$  increases,  $q_b / \gamma B$  tends to converge to a constant value only at  $H/B=0, 1$  and  $2$ . It is generally observed that  $q_b / \gamma B$  tends to converge to a constant value with an increase of  $S/B$ , when  $\phi$  is larger and  $H/B$  is smaller. Regarding the influence of cohesion of the clay, the bearing capacity is increased when  $c_u / \gamma B$  increases from 0.5 to 1.5 for  $\phi = 35^\circ$  in the cases of  $H/B=0, 1, 2, 3$  and  $4$ , as shown in Figs. 7(b) and 8(a). For the cases that  $c_u / \gamma B$

increases from 1.5 to 2.5 for  $\phi = 35^\circ$  (Figs. 8(a) and (b)), the bearing capacities at  $H/B=0, 1$  and  $2$  are significantly increased and those at  $H/B=3$  and  $4$  are slightly increased. Therefore, it is found from Figs. 7 and 8 that the increase of the internal friction angle  $\phi$  in the upper sand layer is more effective than that of the cohesion  $c_u$  in the lower clay, to increase the total bearing capacity in two-layer foundation soils.

## RESULTS AND DISCUSSION

The results of the ultimate bearing capacities calculated by each method are shown based on the internal friction angle  $\phi$  of the upper sand layer, as shown in Figs. 9-11. The horizontal and vertical axes represent  $H/B$  and  $q_b / \gamma B$ , respectively. In each figure, the normalized cohesion  $c_u / \gamma B$  of the clay is increased from (a) to (c). Figure 9 shows the comparisons between  $q_b / \gamma B$  and  $H/B$ , when  $\phi$  is relatively small ( $\phi = 30^\circ$ ). In Figs. 9(b) and (c), the ultimate bearing capacities calculated by Yamaguchi are excessively overestimated in comparison with other methods. When  $c_u / \gamma B$  is increased from (a) to (c) in Fig. 9, the ultimate bearing capacities calculated by Meyerhof tend to be underestimated compared with other methods except FEM. In Fig. 9(a), the ultimate bearing capacities from the upper bound analysis using the failure mechanism for two-layer foundation soils are a little larger than those calculated by Okamura et al., but in Figs. 9(b) and (c), the tendency is opposite. Overall, it is found that the ultimate bearing capacities from the upper bound analysis agree well with those calculated by Okamura et al. in comparison with other methods. Regarding the results from FEM, since the ultimate bearing capacities are increased very little in the cases of  $H/B=3.0$  and  $4.0$  in Fig. 9(b) and  $H/B=2.0, 3.0$  and  $4.0$  in Fig. 9(c), FE analysis tends to evaluate low the ultimate bearing capacities compared to other methods. The reason why the results obtained from FEM evaluate low the ultimate bearing capacities compared with other methods is mainly due to the different assumptions between rigid-plastic and elasto-plastic analyses. Since the failure mechanism needs to be essentially assumed in the limit equilibrium concept and upper bound analysis, the validity of failure mechanism would be very important. This is so because the analytical results are mainly affected by the failure mechanism. In contrast,



Bearing capacity of spread foundations on sand overlying clay

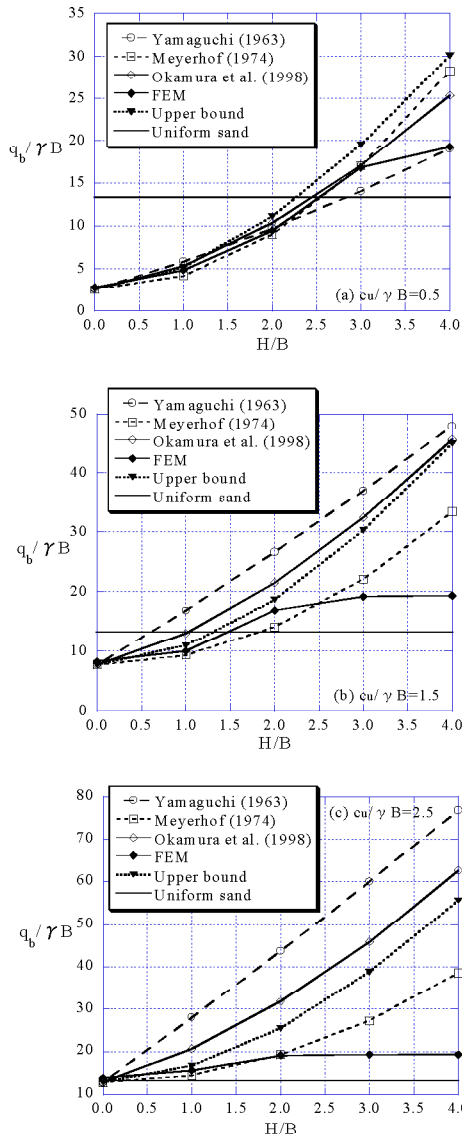


Fig. 9 Comparisons between  $q_b / \gamma B$  and  $H/B$  for  $\phi = 30^\circ$

although the elasto-plastic FE analysis needs many parameters and much computational cost in comparison with rigid-plastic analysis, it would be possible to obtain ultimate bearing capacities more accurately from initial conditions by conducting a careful handling of the sources of error. However, the accuracy and stability of the analysis are very dependent on the discretization of the continuum by finite elements, the selection of an analytical model

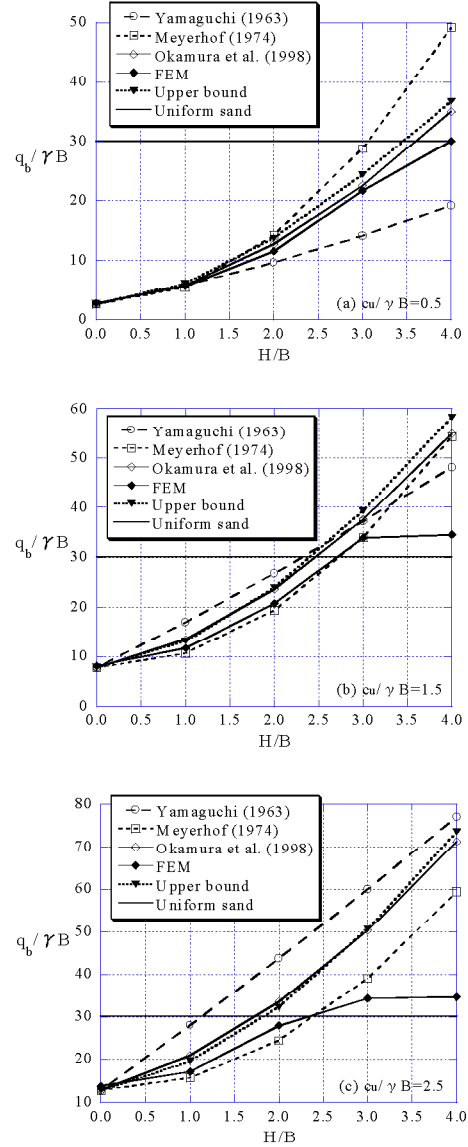


Fig. 10 Comparisons between  $q_b / \gamma B$  and  $H/B$  for  $\phi = 35^\circ$

and the suitability of the method for solving material non-linearity.

The horizontal line shows the upper bound value calculated by the failure mechanism within the uniform sand layer, as shown in Fig. 5(b). As indicated in Fig. 5(b), the lower clay does not affect the failure mechanism within the uniform sand layer. Except for the case that the lower clay is very stiff and  $H/B$  is relatively small, the bearing capacity of

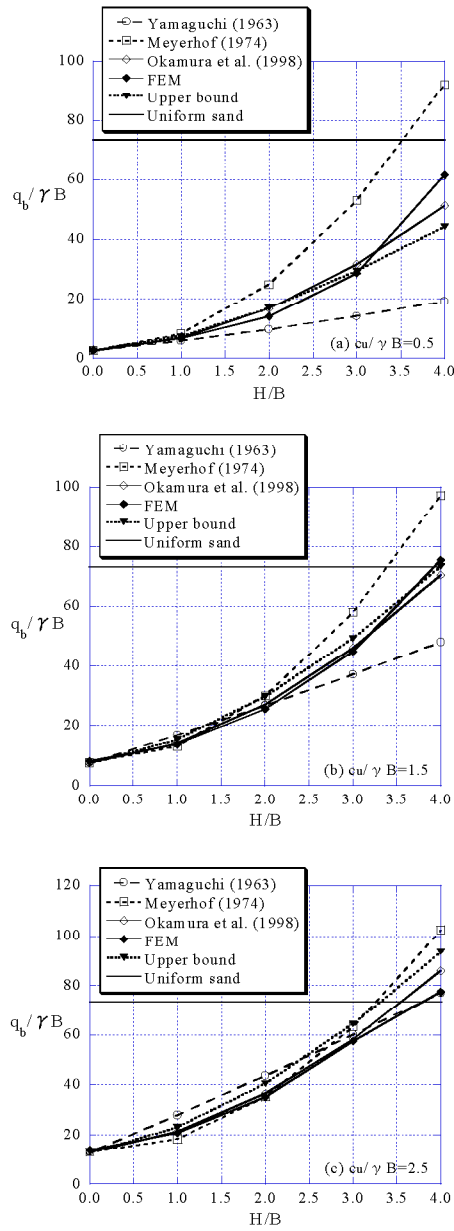


Fig. 11 Comparisons between  $q_b/\gamma B$  and  $H/B$  for  $\phi = 40^\circ$

two-layer foundation soils would not actually exceed that of uniform sand layer. The bearing capacity calculated by the equation using the upper bound method or the limit equilibrium method for two-layer foundation soils continues to increase with the increase of  $H/B$ , as shown in Fig. 9. Thus, we should consider the comparison of bearing capacity obtained

from several methods roughly below the horizontal line, although the horizontal line is the upper bound value from the uniform sand layer. It is found from Fig. 9(c) that the ultimate bearing capacities calculated by all methods for two-layer foundation soils are larger than the upper bound value obtained from uniform sand layer. This indicates that all methods for calculating the bearing capacity of two-layer foundation soils are not applicable to this case, because there is a possibility for overestimating the bearing capacity of two-layer foundation soils.

It is observed in Fig. 10 that the ultimate bearing capacities calculated by Yamaguchi are underestimated compared with other methods in Fig. 10(a), but a different tendency is found in Fig. 10(c). With an increasing sand layer, the ultimate bearing capacities calculated by Meyerhof tend to be overestimated compared with other methods in Fig. 10(a), but the opposite tendency is shown in Fig. 10(c). The ultimate bearing capacities from the upper bound analysis using the failure mechanism for two-layer foundation soils show good agreement with those calculated by Okamura et al. In the cases of  $H/B=3.0$  and  $4.0$  in Figs. 10(b) and (c), the ultimate bearing capacities from FEM are almost the same. Thus, the results from FEM tend to evaluate low the ultimate bearing capacity compared to other methods. Additionally, it is confirmed that the failure mechanism around the foundation is almost the same at  $H/B=3.0$  as at  $4.0$  in Figs. 10(b) and (c), respectively. It is seen from Figs. 9-10(b) and (c) that the ultimate bearing capacities obtained from FEM are a little larger than the upper bound value obtained from the uniform sand layer for the cases of  $H/B \geq 2.0$  in Figs. 9(b) and (c) and  $H/B \geq 3.0$  in Figs. 10(b) and (c). The reason is depend on the assumption of the failure mechanism within the uniform sand layer used in limit analysis, as shown in Fig. 5(b) and the determination of ultimate bearing capacity in the load-settlement curve obtained from FEM. For the load-settlement curve that does not tend to converge to a constant value, if the point given by the intersection of tangents to the initial and ultimate portions of the curve is adopted as a ultimate bearing capacity, it is possible to evaluate low the ultimate bearing capacity than that at  $S/B=0.15$ .

Figure 11 shows comparisons between  $q_b/\gamma B$  and  $H/B$ , when  $\phi$  is relatively large ( $\phi = 40^\circ$ ). At  $H/B \geq 3.0$  in Figs. 11(a) and (b), the ultimate bearing capacities calculated by Yamaguchi tend to be

underestimated compared with other methods. Meyerhof's solutions tends to overestimate excessively the ultimate bearing capacities at  $H/B \geq 2.0$  in Fig. 11(a) and  $H/B \geq 3.0$  in Fig. 11(b). In this figure, it is seen that the upper bound solutions using the failure mechanism for two-layer foundation soils agree well with those calculated by Okamura et al. among the various methods. Notice that the ultimate bearing capacities obtained from FEM are larger than the upper bound solutions only at  $H/B=4.0$  in Figs. 11(a) and (b). This is because of the determination of ultimate bearing capacity in the load-settlement curve obtained from FEM. It is seen that the tendency of the results obtained from FEM in Fig. 11 is different from that in Figs. 9 and 10. This may be due to the fact that the bearing capacity failure of two-layer foundation soils mainly takes place in the upper hard sand layer ( $\phi = 40^\circ$ ), thus the ultimate bearing capacities are increased due to the easy propagation of the failure. It is found from Figs. 9-11 that the application range (the region below the horizontal line) of the bearing capacity equation for two-layer foundation soils becomes large as  $\phi$  increases and  $c_u/\gamma B$  reduces.

Therefore, although the upper bound solutions, i.e., minimum bearing capacities calculated by Eqs. (2)-(4) for the two-layer foundation soils and Eqs. (7)-(8) for the uniform sand layer give the upper bound values of the true ultimate bearing capacity, it is considered that the upper bound solutions from two failure mechanisms (Figs. 5(a) and (b)) proposed in this paper can obtain relatively good values for the analytical conditions shown in Fig. 4, comparing with other methods. Upper bound solutions, in contrast to limit equilibrium methods, do not need to introduce certain concepts or assumptions, the necessary parameters are simple and the theoretical background is reasonable. The design charts from the upper bound solutions obtained are described below for practice use.

Figure 12 shows the relationship between  $q_b/\gamma B$  and  $c_u/\gamma B$  for  $\phi = 30^\circ$ ,  $35^\circ$  and  $40^\circ$  from the upper bound analysis. As the horizontal line shows the upper bound value calculated by the failure mechanism within the uniform sand layer, the application range of the upper bound values obtained from the failure mechanism of two-layer foundation soils is roughly below the horizontal line. The upper bound values beyond the horizontal line are also not applicable, because these values exceed the upper

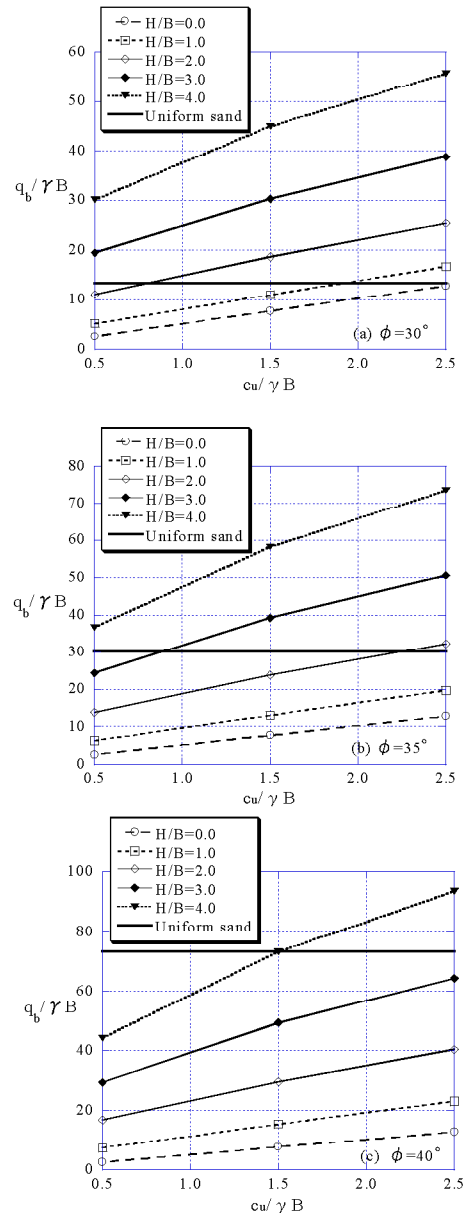


Fig. 12 Relationship between  $q_b/\gamma B$  and  $c_u/\gamma B$  for various friction angles from upper bound analysis

bound values from the uniform sand layer. It is found that the application range is very small for  $\phi = 30^\circ$  and becomes large when  $\phi$  increases. Regarding the estimation of the bearing capacity of two-layer foundation soils from limit analysis, it is considered that the smaller value of bearing capacities calculated

by the failure mechanism of the two-layer foundation soils (Fig. 5(a)) or calculated by that of the uniform sand layer (Fig. 5(b)) should be adopted as a simplified calculation. In addition, when the upper bound solution from the failure mechanism within the uniform sand layer is obtained, the normalized depth of the failure mechanism  $H/B$  is less than 2 for  $\phi = 30^\circ$ ,  $35^\circ$  and  $40^\circ$ . When the internal friction angle  $\phi$  of the upper sand layer and the normalized cohesion  $c_u/\gamma B$  of the lower clay are known, the upper bound value of the true ultimate bearing capacity can be readily obtained using these design charts. Notice that the condition  $H/B=0$  indicates the case of only a clay soil.

Figure 13 shows the variation of the load spreading angle  $\alpha$  with the normalized cohesion  $c_u/\gamma B$  from the upper bound analysis. The angle  $\alpha$  in the failure mechanism of two-layer foundation soils increases with increasing internal friction angle  $\phi$  in the upper sand layer, and the angle decreases when  $c_u/\gamma B$  of the lower clay increases. In particular, the decrease of the angle from  $c_u/\gamma B=0.5$  to 1.5 is more remarkable than that from  $c_u/\gamma B=1.5$  to 2.5, irrespective of  $H/B$  and  $\phi$ . It is also found that the angle is the largest for  $H/B=4$  and is the smallest for  $H/B=1$  among all cases.

CONCLUSIONS

The ultimate bearing capacity of a rigid spread foundation with rough base on a sand layer overlying clay was investigated using the upper bound analysis, the finite element program (ABAQUS) and existing finite limit equilibrium methods. The ultimate bearing capacities obtained from the upper bound analysis and the program ABAQUS were compared with those calculated from some limit equilibrium equations proposed by Yamaguchi (1963), Meyerhof (1974) and Okamura et al. (1998) for confirming the validity of their application to practice.

The conclusions drawn from this study are summarized as follows:

1. The ultimate bearing capacities calculated by Yamaguchi (1963) are largely influenced by an increase of  $c_u/\gamma B$  and are not dependent on an increase of  $\phi$  at all. Meyerhof's solutions tends to underestimate or overestimate bearing capacity for the condition of  $H/B \geq 3.0$ , compared with those calculated by the other methods. Therefore, it can be concluded that Yamaguchi's and Meyerhof's

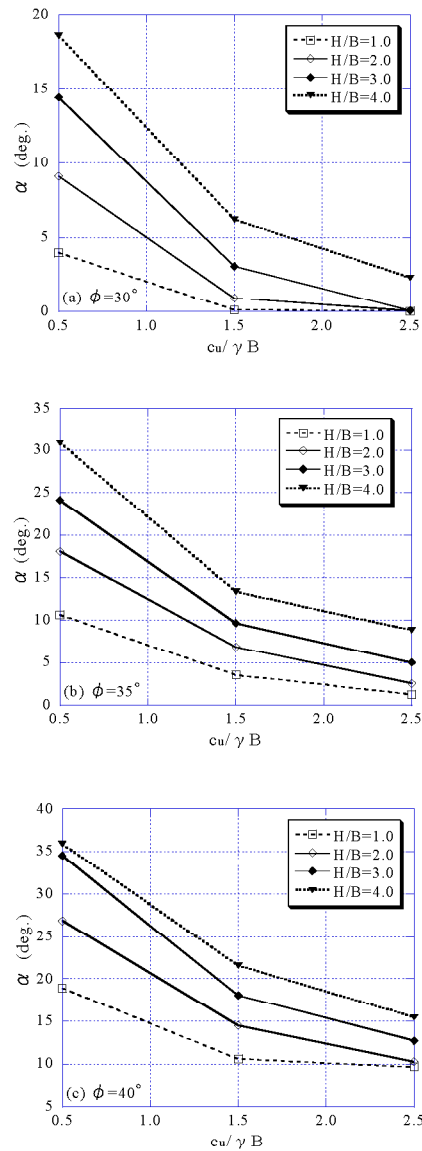


Fig. 13 Variation of  $\alpha$  with  $c_u/\gamma B$  from upper bound analysis

solutions are inadequate for estimating the ultimate bearing capacity, because their solutions are not consistent with varying conditions in two-layer foundation soils.

2. The ultimate bearing capacities calculated by Okamura et al. (1998), regarded to be the most accurate of the considered equations showed good agreement with the upper bound solutions. Within the

bearing capacity obtained from the failure mechanism of two-layer foundation soils does not exceed that calculated by the failure mechanism of the uniform sand layer, the authors suggest that the upper bound solutions or Okamura et al.'s solution should be applied for the estimation of bearing capacity in practice (noting that their solutions may overestimate the true ultimate bearing capacity).

3. The bearing capacity equation was proposed by the kinematic approach of limit analysis and the upper bound solutions were shown in the form of design charts. Using these design charts, when the internal friction angle  $\phi$  of the upper sand layer and the normalized cohesion  $c_u/\gamma B$  of the lower clay are known, the true ultimate bearing capacity can be reasonably estimated with ease.

4. From the load spreading angle  $\alpha$  in the failure mechanism of two-layer foundation soils used in the upper bound analysis, the upper sand layer is more effective for spreading the footing load when  $\phi$  increases and  $c_u/\gamma B$  reduces. Therefore, it is considered that fixing the load spreading angle for various soil conditions is unfavorable for some practical applications. In addition, it is very difficult to estimate the load spreading angle in advance.

5. Although the bearing capacity calculated by the equation using the upper bound method or the limit equilibrium method in this paper continues to increase with the increase of  $H/B$ , only FE analysis can indicate the limit of the increase of bearing capacity corresponding to the increase of  $H/B$  without introducing concepts or assumptions.

#### REFERENCES

- Burd, H. J. and Frydman, S. (1997). Bearing capacity of plane-strain footings on layered soils. *Can. Geotech. J.* 34: 241-253.
- Burd, H. J. and Frydman, S. (1999). Discussion on 'The bearing capacity of footings on a sand layer overlying soft clay' by M. J. Kenny and K. Z. Andrawes. *Geotechnique*. 49(4): 554-555.
- Chen, W. F. (1975). *Limit analysis and soil plasticity*. Elsevier, Amsterdam.
- Chen, W. F. and Liu, X. L. (1990). *Limit analysis in soil mechanics*. Elsevier, Amsterdam.
- Chen, W. F. and Saleeb, A. F. (1994). *Constitutive Equations for Engineering Materials*, Vol. 2. Elsevier Science B.V., Amsterdam.
- Desai, C. C. and Siriwardane, H. J. (1984). *Constitutive Laws for Engineering Materials with Emphasis on Geological Materials*. Prentice-Hall, New Jersey.
- Hanna, A. M. and Meyerhof, G. G. (1980). Design charts for ultimate bearing capacity of foundations on sand overlying soft clay. *Can. Geotech. J.* 17: 300-303.
- Hanna, A. M. (1981). Foundations on strong sand overlying weak sand. *J. Geotech. Engrg. Div. ASCE*. 107(GT7): 915-927.
- HKS. (2001). ABAQUS/standard, a general purpose finite element code. Hibbit, Karlsson & Sorensen.
- Kenny, M. J. and Andrawes, K. Z. (1997). The bearing capacity of footings on a sand layer overlying soft clay. *Geotechnique*. 47(2): 339-345.
- Kraft, L. M. and Helfrich, S. C. (1983). Bearing capacity of shallow footing, sand over clay. *Can. Geotech. J.* 20: 182-185.
- Meyerhof, G. G. (1974). Ultimate bearing capacity of footings on sand layer overlying clay. *Can. Geotech. J.* 11(2): 223-229.
- Michalowski, R. L. and Shi L. (1995). Bearing capacity of footings over two-layer foundation soils. *J. Geotech. Engrg. Div. ASCE*. 121(5): 421-428.
- Mizuno, K. and Tsuchida, T. (2002). Practical use of finite element analysis for slope stability and bearing capacity. *Proc. of Foundation design codes and soil investigation in view of international harmonization and performance*, Kamakura.: 359-367.
- Okamura, M., Takemura, J. and Kimura, T. (1997). Centrifuge model tests on bearing capacity and deformation of sand layer overlying clay. *Soils Found.* 37(1): 73-88.
- Okamura, M., Takemura, J. and Kimura, T. (1998). Bearing capacity predictions of sand overlying clay based on limit equilibrium methods. *Soils Found.* 38(1): 181-194.
- Terzaghi, K. (1943). *Theoretical soil mechanics*. John Wiley & Sons, New York.
- Yamaguchi, H. (1963). Practical formula of bearing value for two layered ground. *Proc. of 2rd ARCSMFE*. 1: 176-180.